A novel subset of putative stem/progenitor CD34+Oct-4+ cells is the major target for SARS coronavirus in human lung

Yongxiong Chen,[1,4] Vera Sau-Fong Chan,[1,4] Bojian Zheng,[2] Kelvin Yuen-Kwong Chan,[3] Xiaoning Xu,[6] Leo Yuk-Fai To,[1,4] Fang-Ping Huang,[5] Ui-Soon Khoo,[3] and Chen-Lung Steve Lin[1,4]

[1]Department of Surgery, [2]Department of Microbiology, and [3]Department of Pathology, Li Ka Shing Faculty of Medicine, The University of Hong Kong, Hong Kong SAR, China
[4]Division of Surgery, Oncology, Reproductive Biology and Anaesthetics, Faculty of Medicine, and [5]Department of Molecular Genetics and Rheumatology, Division of Medicine, Imperial College London, Hammersmith Hospital, London W12 0NN, UK
[6]Human Immunology Unit, The Weatherall Institute of Molecular Medicine, University of Oxford, Oxford OX3 9DS, UK

Identification of the nature of severe acute respiratory syndrome (SARS)-infected cells is crucial toward understanding the pathogenesis. Using multicolor colocalization techniques, we previously reported that SARS+ cells in the lung of fatally infected patients expressed the only known functional receptor, angiotensin-converting enzyme 2, and also a binding receptor, liver/lymph node–specific ICAM-3–grabbing non-integrin (CD209L). In this study, we show that SARS-infected cells also express the stem/progenitor cell markers CD34 and Oct-4, and do not express cytokeratin or surfactant. These putative lung stem/progenitor cells can also be identified in some non-SARS individuals and can be infected by SARS-coronavirus ex vivo. Infection of these cells may contribute to the loss of lung repair capacity that leads to respiratory failure as clinically observed.

CORRESPONDENCE
Chen-Lung Steve Lin:
steve.lin@imperial.ac.uk

SARS is an acute respiratory disease from infection of a novel coronavirus (SARS-CoV) that spreads mainly through the respiratory route (1–3), with angiotensin-converting enzyme 2 (ACE2) as the only known functional receptor (4). One of the clinical features in SARS infection is continuous deterioration of lung function and the obvious loss of lung repair capacity after viral load has declined (5). However, the pathogenesis for SARS-CoV infection, for which characterizing the nature of virus-infected cells is crucial, is still ill-defined. Reports in the literature regarding the identity of SARS+ cells are unconvincing either because no colocalization study was performed or because of technical limitations. Results in the literature are also inconsistent in that some reports suggested type I pneumocytes, whereas others suggested type II pneumocytes, as the major target in humans and in simian models (6–11). It has also been implied that these SARS+ cells express cytokeratin, whether they are described as type I or type II cells (6–10, 12). It is also a concern that none of these reports demonstrated colocalization of ACE2 expression with SARS-infected cells. Using multicolor colocalization techniques, we previously reported that cells containing SARS-CoV antigen in the autopsy lung of SARS patients expressed ACE2 and liver/lymph node–specific ICAM-3–grabbing non-integrin (L-SIGN; CD209L) (13). L-SIGN is a SARS-CoV binding receptor that mediates proteasome-dependent viral degradation and is expressed in cytokeratin+ respiratory epithelia (Fig. S1, available at http://www.jem.org/cgi/content/full/jem.20070462/DC1) (13). L-SIGN can also facilitate SARS-CoV infection/replication in trans (13). In this study, we further characterize the SARS-infected cells and show that a novel subset of putative stem/progenitor CD34+Oct-4+ cells are the only cells expressing ACE2 in the human lung and are the major target for SARS-CoV infection.

RESULTS AND DISCUSSION

SARS+ cells in alveoli and terminal bronchioles do not express cytokeratin or surfactant

To characterize the phenotype of SARS+ cells, autopsy lung samples from nine SARS patients

Y. Chen and V.S.-F. Chan contributed equally to this work.
The online version of this article contains supplemental material.

were subjected to triple-color sequential immunohistochemistry (IHC) and immunofluorescence staining on the same section. We found that the SARS antigen could be detected in six patients who died within 11 d after illness onset, but not in the other three patients who died 21, 24, or 27 d after disease onset (Table I), which is consistent with a recent report showing that SARS antigen or RNA could not be detected in patients who died >2 wk after disease onset (11). In samples where SARS antigen was detected, as many as 42 SARS$^+$ cells in a microscopic field (400×) were identified (Table I). By location, SARS$^+$ cells were found in the alveoli (Fig. 1, a and b, and d and e, red) and the bronchiolar lining layer (Fig. 1, j and k, red). By morphology, SARS$^+$ cells were round or oval in shape and rich in cytoplasm (Fig. 1, b, d, e, j, and k). Furthermore, SARS$^+$ cells did not express surfactant A, a type II pneumocyte marker (Fig. 1, a, b, d, and j, brown), or cytokeratin (Fig. 1, e and k, green). SARS$^+$ cells did not express surfactant C (also a type II pneumocyte marker) or T1α (a type I pneumocyte marker) either (Fig. S2, available at http://www.jem.org/cgi/content/full/jem.20070462/DC1). Because bronchial/bronchiolar lining layers are composed of multiple cell types that are compactly arranged, some SARS$^+$ cells were "overlapping" with adjacent cytokeratin$^+$ cells (e.g., one indicated by a circle, Fig. 1 k and Fig. S3), which could be mistakenly interpreted as "colocalized" on two-dimensional images. However, they could be carefully distinguished by adjusting the focus under the microscope.

Our findings indicate that SARS-infected cells are unlikely to be pneumocytes (either type 1 or type 2) or cytokeratin$^+$ epithelial cells. This observation is supported by a recent report that SARS-CoV cannot infect or replicate in the fully differentiated mouse type 1 or type 2 pneumocytes (14). Our result does contradict some data in the literature that suggest that cytokeratin$^+$, surfactant$^+$, or the epithelial membrane antigen–expressing pneumocytes are targeted by SARS-CoV (6–12). Upon reviewing the literature, however, we noticed that in

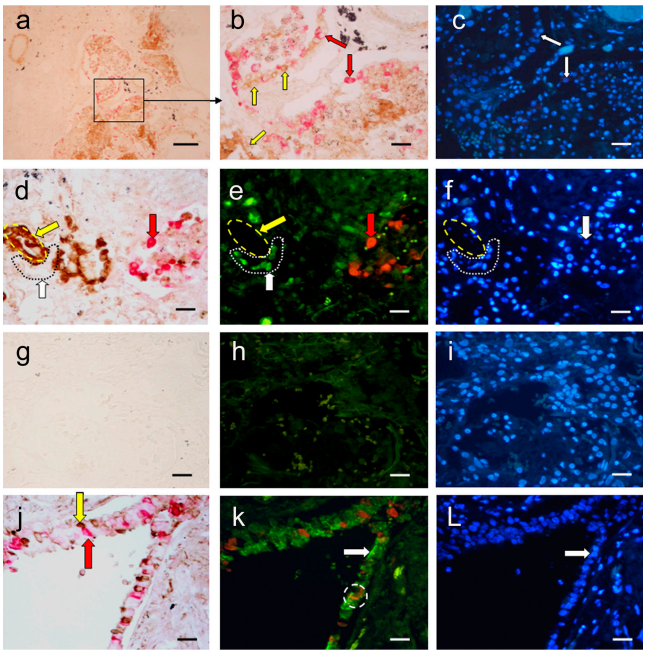

Figure 1. SARS$^+$ cells do not express cytokeratin or surfactant in alveoli (a–f) and terminal bronchioles (j–L). SARS lung autopsy samples studied by IHC for surfactant A (brown labeling in a, b, d, and j; some indicated by yellow arrows), for SARS-CoV nucleocapsid antigen (red labeling; some indicated by red arrows in a, b, d, and j; also visible in e and k), and immunofluorescence for cytokeratin (green labeling in e and k; some indicated by white arrows). The black circle in d indicates where cytokeratin$^+$ cells are visualized in e. The yellow circle in e indicates where surfactant$^+$ cells are visualized in d. DAPI counterstaining showing the cellular nuclei is in the right column. Isotype antibody control for IHC and immunofluorescence is in g and h, respectively. Some SARS$^+$ cells were actually "overlapping" with adjacent cytokeratin$^+$ cells (one indicated by a circle in k), which might be mistakenly regarded "colocalized" on two-dimensional photos. Panels of each row represent results of the same section from a patient. Results are representative of six SARS patients who died within 11 d after disease onset. Bar, 20 μm.

Table I. Number of SARS$^+$ cells in fatally infected SARS lung

Case no.	Age (years)/Sex	Mortality date (days after illness onset)	SARS$^+$ cell[a] mean ± SD (range)	Phenotype of SARS$^+$ cells	
				CD34$^+$	CD34$^-$ (range)
1	69/M	4	10 ± 3 (6–13)	9 ± 3 (6−12)	0–1
2	80/F	5	21 ± 14 (9–42)	19 ± 13 (9−39)	0–4[b]
3	91/F	9	7 ± 3 (5–12)	7 ± 3 (5−12)	*Nil*
4	64/M	9	6 ± 3 (4–11)	6 ± 3 (4−11)	*Nil*
5	76/M	11	5 ± 2 (3–8)	5 ± 2 (3−8)	*Nil*
6	95/F	11	3 ± 1 (2–4)	3 ± 1 (2−4)	*Nil*
7	37/F	21	*Nil*	–	–
8	71/M	24	*Nil*	–	–
9	47/M	27	*Nil*	–	–

No SARS antigen could be detected in patients 7–9. *Nil*, no detectable SARS$^+$ cells in at least 20 fields (400×) of each lung sample.
[a]Numbers were obtained by counting SARS$^+$ cells from five different fields (400×) of lung samples in patients 1–6.
[b]Including 0–1 SARS$^+$CD68$^+$ cell per field.

some of previous reports the identity of the SARS$^+$ cells was judged by morphology or location alone without colocalization with specific markers to confirm the phenotype (6, 7, 10). In addition, these reports used avidin–biotin complex for SARS-CoV or cytokeratin staining (6, 7, 10). Biotin is widely dispersed in mammalian tissues (15–17), and the presence of endogenous biotin is likely to result in false-positive readings, even after blocking procedures before immunodetection (18). Experiences with this problem have also been encountered in our lab (Fig. S4, available at http://www.jem.org/cgi/content/full/jem.20070462/DC1). In other reports, the double-color results for colocalization either could not be clearly differentiated from single-color staining (8, 9) or were interfered by autofluorescence (11, 12) or by hematoxylin counterstaining (9). It is also a concern that none of these reports demonstrates the colocalization of ACE2 expression with the SARS$^+$ cells. Interpretation of these reports thus requires reappraisal.

SARS$^+$ cells express the functional receptor ACE2 and markers for stem/progenitor cells

Because SARS$^+$ cells did not express cytokeratin or surfactant A (Fig. 1), we investigated if the SARS$^+$ cells might be leukocytes infiltrating in the lung. Results showed that the SARS$^+$ cells did not express tryptase, defensins 1/2/3, CD15, CD68, CD57, CD45RO, CD3, and CD20, indicating that they were not mast cells, neutrophils, macrophages/monocytes, NK, T, or B cells (Fig. S5, available at http://www.jem.org/cgi/content/full/jem.20070462/DC1). We next examined the markers for other cell types. CD34 is expressed by hematopoietic progenitors in the circulation (19) and also by bone marrow stromal cell precursors (20). By a four-color sequential IHC and simultaneous fluorescence in situ hybridization (FISH) and ISH study, we demonstrated that SARS$^+$ cells (Fig. 2 a, red) were distinct from cells expressing the macrophage/monocyte-specific marker CD68 (Fig. 2 a, brown), and the SARS$^+$ cells expressed the only known functional receptor ACE2 (Fig. 2 b, green) as well as the stem/progenitor cell marker CD34 (Fig. 2 c, purple). Similar observations were made in the bronchioles, i.e., SARS$^+$ cells expressed both ACE2 and CD34 (Fig. S6). In a separate sequential IHC/FISH/ISH study, SARS$^+$ cells (Fig. 2 i, red) expressed CD34 (Fig. 2 j, green) and another stem/progenitor cell marker, Oct-4 (Fig. 2 k, purple). Oct-4 is a transcription factor, and its activity is essential for maintaining pluripotency of the

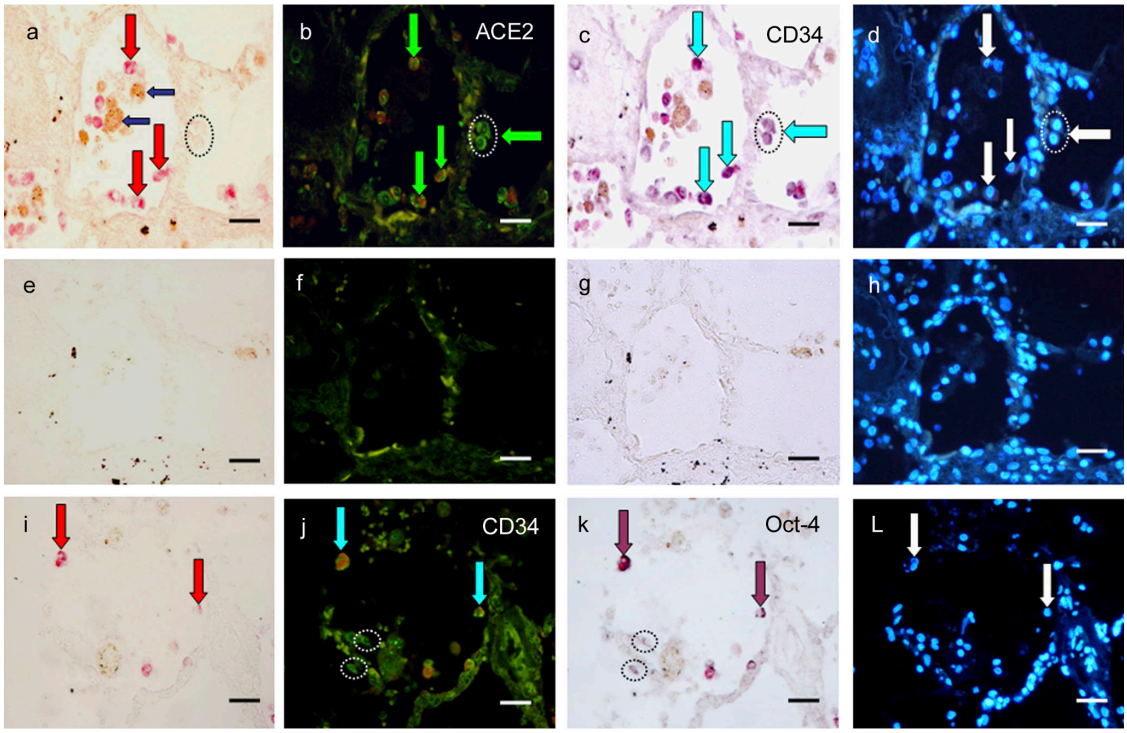

Figure 2. SARS$^+$ cells in the alveoli express ACE2, CD34, and Oct-4. (a–c) IHC on SARS autopsy lung for CD68 (brown labeling, some indicated by dark blue arrows in a) and for SARS-CoV antigen (red labeling, some indicated by red arrows in a; also visible in b and c), followed by FISH for ACE2 (green labeling in b, some indicated by green arrows and a circle) and ISH for CD34 (purple labeling in c, some indicated by light blue arrows and a circle). Circles in a, b, and c indicate uninfected ACE2$^+$CD34$^+$ cells. (e–g) Isotype antibody control for IHC, ACE2 sense control for FISH, and CD34 sense control for ISH, respectively. (i–k) IHC for SARS-CoV antigen (red labeling, some indicated by red arrows in i; also visible in j and k), followed by FISH for CD34 (green labeling in j, some indicated by light blue arrows and circles), and ISH for Oct-4 (purple labeling in k, some indicated by purple arrows and circles). Circles in j and k indicate uninfected CD34$^+$Oct-4$^+$ cells. Isotype antibody control for IHC, CD34 sense control for FISH, and Oct-4 sense control for ISH are similar to e, f, and g, respectively (not depicted). DAPI counterstaining is in the right column. Panels of each row represent results on the same section of a patient. Results are representative of six SARS patients. Bar, 20 μm.

mammalian embryonic cells (21, 22). Such observations were made in all lung samples from patients recruited for this study who died within 11 d after illness onset (Table I). We thus conclude that the majority of SARS$^+$ cells in the SARS lung were a subset of putative stem/progenitor cells expressing CD34, Oct-4, and ACE2.

It is noteworthy although SARS antigen could not be detected in most CD68$^+$ cells (Fig. 2 a and Fig. S5), SARS$^+$CD68$^+$ cells were occasionally found in selected sections of a patient (Table I and Fig. S7, available at http://www.jem.org/cgi/content/full/jem.20070462/DC1). However, in contrast to the diffusely intra-cytoplasmic staining in SARS$^+$CD34$^+$ cells, the viral staining in CD68$^+$ cells was usually granular (Fig. 2 a vs. Fig. S7), suggesting that the mechanism(s) by which SARS antigen enters CD34$^+$ and CD68$^+$ cells may be different. Because CD68$^+$ cells did not express the functional receptor ACE2 (Fig. 2), we regard that the presence of viral antigen in CD68$^+$ cells is most likely due to phagocytosis.

ACE2$^+$CD34$^+$Oct-4$^+$ cells are present in non-SARS lung and express L-SIGN, and can be infected by SARS-CoV ex vivo

To determine if ACE2$^+$CD34$^+$Oct4$^+$ cells could be found in non-SARS lung, lung tissues from 14 lung cancer patients who had no SARS infection (Table II) were examined. Eight of these patients were retrieved from our archive. The other six were additionally enrolled to obtain fresh lung tissues, part of which was immediately fixed, embedded, and sectioned for IHC-FISH-ISH study upon collection, and the other part was used for ex vivo infection experiments (described below). Results showed that ACE2 signals were detectable in samples from 8 of 14 lung cancer patients, but not in the others (Table II). In these eight patients, we found that consistent with our findings in the SARS lung, ACE2 (Fig. 3 A, b, f, and n, green) was not expressed by surfactant A$^+$ cells (Fig. 3 A, a, e, i, and m, brown; each row represents results from a patient) but was expressed by CD34$^+$ cells (Fig. 3 A, c and j, purple or green). For better differentiation between alveolar and vascular lumens, an endothelial cell marker, CD31, was used to depict blood vessels (Fig. 3 A, a–c, red). We showed that cytokeratin$^+$ cells (Fig. 3 A, e, f, m, and n, red) did not express ACE2 either (Fig. 3 A, f and n, green). Furthermore, CD34 expression (Fig. 3 A, j, green) was colocalized with Oct-4 (Fig. 3 A, k, purple). Interestingly, these ACE2$^+$CD34$^+$Oct4$^+$ cells did not express CD15 (i.e., SSEA-1), another marker for stem/progenitor cells (Fig. 3 A, i, j, and k, red). We also found that in line with our previous report (13), ACE2$^+$ cells (Fig. 3 A, n, green) also expressed L-SIGN (Fig. 3 A, p, purple), a binding receptor for SARS-CoV. In the lung samples from these eight patients, the number of CD34$^+$ cells was identified from 2 to 72 per microscopic field (400×) (Table II). Therefore, ACE2$^+$CD34$^+$Oct4$^+$L-SIGN$^+$ cells are also present in the lung of some non-SARS individuals. Together with our previous findings (reference 13 and Fig. S1), we also conclude that the binding receptor L-SIGN is expressed by at least two cell types in the non-SARS lung: cytokeratin$^+$ACE2$^-$ bronchial/bronchiolar epithelial cells and CD34$^+$Oct4$^+$ cells that express ACE2 but not cytokeratin; however, only the latter contain SARS-CoV antigen in the SARS lung. We also note that the frequency of CD34$^+$ cells in the non-SARS lung appears to be higher than that of SARS$^+$ cells in the SARS samples. However, these numbers cannot be directly compared because the non-SARS lung samples were from lung cancer patients, which may not represent the situations in healthy individuals who have no lung pathology. Furthermore, it is still unclear how the frequency of these putative stem/progenitor cells is regulated, for example, in cancers.

To further investigate if CD34$^+$ cells in the non-SARS lung could be infected by SARS-CoV, part of the fresh lung tissue collected from six lung cancer patients (Table II) was cut into small blocks (2–3 mm^3) and directly exposed to live virus as similarly described by others (23). After 16 h, the ex vivo–infected tissue blocks were fixed and embedded for IHC-FISH-ISH study. Results showed that though few in number, SARS$^+$ cells were identified in samples from four patients (Fig. 3 B, b and c, red, and Figs. S8 and S9, which are available at http://www.jem.org/cgi/content/full/jem.20070462/DC1). Consistently, these four patients also had detectable CD34$^+$ Oct-4$^+$ cells in the fresh samples studied immediately upon collection (Table II). Furthermore, in line with observations in the SARS-infected lung, the SARS antigen (Fig. 3 B, b and c, red, and Fig. S8) was not colocalized with surfactant A (Fig. 3 B, b, brown, and Fig. S8). SARS$^+$ cells could be clearly visualized under a fluorescence microscope before FISH study (Fig. 3 B, c). After FISH/ISH study, SARS$^+$ cells indeed

Table II. Numbers of CD34$^+$ cells in lung samples from lung cancer patients

Case no.	Age (years)/Sex	Numbers[a] mean ± SD (range)
1	68/M	10 ± 8 (2–22)
2	67/M	18 ± 17 (4–45)
3	67/M	*Nil*
4	70/F	*Nil*
5	52/M	40 ± 5 (35–48)
6	55/M	*Nil*
7	54/M	22 ± 12 (6–38)
8	72/F	*Nil*
9[b]	77/M	55 ± 15 (40–72)
10[b]	64/M	34 ± 5 (28–40)
11[b]	79/M	24 ± 17 (6–40)
12[b]	71/F	*Nil*
13[b]	40/M	20 ± 10 (11–36)
14[b]	49/M	*Nil*

Patients 1–8 were from the archive. Patients 9–14 were recruited for ex vivo infection, and IHC-FISH-ISH study was performed in each sample before and after ex vivo infection. CD34$^+$ cells express Oct-4, ACE2, and L-SIGN. *Nil*, no detectable CD34$^+$ cells in at least 20 fields (400×) of each lung sample.
[a]Numbers were obtained by counting CD34$^+$ cells from five different fields (400×) of lung samples from eight lung cancer patients.
[b]Patients selected for ex vivo infection.

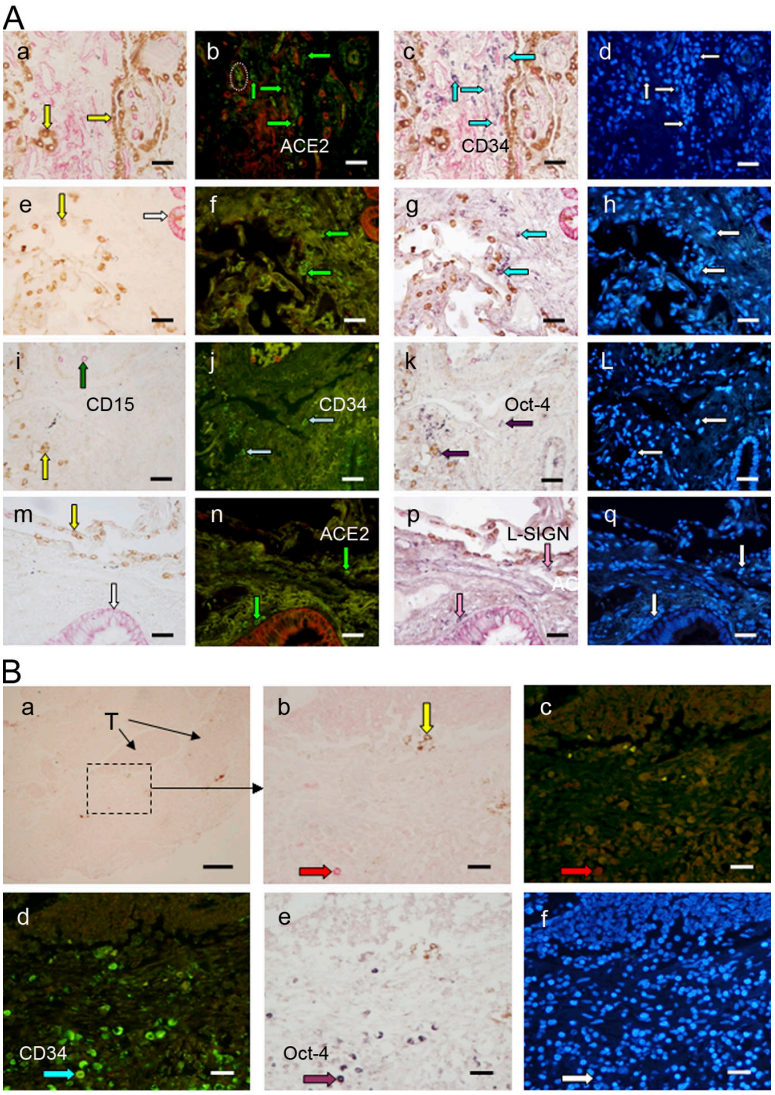

Figure 3. ACE2$^+$CD34$^+$Oct-4$^+$L-SIGN$^+$ cells are present in non-SARS lung and can be infected by SARS CoV ex vivo. (A, a–d) IHC on non-SARS lung samples for surfactant A (brown labeling, some indicated by yellow arrows in a; also visible in c), CD31 (red labeling in a; also visible in b and c), followed by FISH for ACE2 (green labeling in b, some indicated by green arrows) and ISH for CD34 (purple labeling in c, some indicated by light blue arrows). DAPI counterstaining is in d. Circle in b indicates autofluorescence from red blood cells. (e–h) IHC for surfactant A (brown labeling, one indicated by a yellow arrow in e; also visible in g) and for cytokeratin (red labeling, one indicated by a white arrow in e; also visible in f and g), followed by FISH for ACE2 (green labeling in f, some indicated by green arrows) and ISH for CD34 (purple labeling in g, some indicated by light blue arrows). DAPI counterstaining is in h. (i–L) IHC for surfactant A (brown labeling in i, one indicated by a yellow arrow; also visible in k) and for CD15 (red labeling, one indicated by a dark green arrow in i; also visible in j and k), followed by FISH for CD34 (green labeling in j, some indicated by light blue arrows) and ISH for Oct-4 (purple labeling in k, some indicated by purple arrows). DAPI counterstaining is in L. One of the CD34$^+$Oct-4$^+$ cells is juxtaposed to a surfactant$^+$ cell (the yellow arrow in i vs. the lower light blue arrow in j and the lower purple arrow in k). (m–q) IHC for surfactant A (brown labeling, one indicated by a yellow arrow in m; also visible in p) and for cytokeratin (red labeling, one indicated by a white arrow in m; also visible in n and p), followed by FISH for ACE2 (green labeling, some indicated by green arrows in n) and ISH for L-SIGN (purple labeling, some indicated by pink arrows in p). DAPI counterstaining is in q. Some of the ACE2$^+$CD34$^+$Oct4$^+$L-SIGN$^+$ cells are close to surfactant A$^+$ cells (g and k) or cytokeratin$^+$ cells (p). Panels of each row represent results on the same section of a patient. Results are representative of eight patients with lung cancer. Bar, 20 μm. (B) Fresh lung tissues resected from cancer patients were cut into small blocks, exposed to SARS-CoV for 16 h, and studied by IHC for surfactant A (brown labeling in a and b, one indicated by a yellow arrow in b; also visible in e), for SARS antigen (red labeling, indicated by a red arrow in b; also visible in c), followed by FISH for CD34 (green labeling, one indicated by a light blue arrow in d) and ISH for Oct-4 (purple labeling, one indicated by a purple arrow in e). T, tumor. DAPI counterstaining is in f. Results are representative in four of six individuals enrolled. No CD34$^+$ cells could be detected in samples from the other two individuals. Bars: a, 100 μm; b–f, 20 μm.

expressed both CD34 and Oct-4 (Fig. 3 B, d and e, green and purple, respectively, and Fig. S8). In separate sections, triple-color staining confirmed that no cytokeratin or surfactant expression was colocalized with SARS antigen (Fig. S9).

In the ex vivo–infected samples where $SARS^+$ cells were detected, an average of about two to three $SARS^+$ cells per tissue section could be identified. The reason for few cells being infected in this model is unclear. One possibility is that, unlike the in vivo situation where the virus can reside and replicate in the lung for days to weeks, fresh lung tissues in the form of blocks were exposed to live virus for 16 h only. Thus, the virus may not be able to "see" all of these target cells. It is also possible and remains to be investigated if these putative stem/progenitor cells represent a heterogeneous population that is still differentiating and only cells at a certain differentiation stage are susceptible to the viral infection.

Collectively, we conclude that the major target for SARS-CoV in the SARS-infected lung is a novel subset of putative lung stem/progenitor $CD34^+Oct4^+$ cells (Fig. 2), which is also the only cell subset in the fresh non-SARS samples being infected after ex vivo infection (Fig. 3 B). Interestingly, not all of our enrolled non-SARS individuals had detectable putative stem/progenitor cells in the lung. A recent report has shown that approximately one third of SARS-infected patients had self-limited symptoms with no clinical or radiological evidence of progression to pneumonitis, whereas the remaining had progressive deterioration with impaired lung function (24). Whether or not our findings may contribute to the above clinical observation deserves further study. It also remains to be investigated if these putative stem/progenitor cells also exist in nasopharynx, throat, or trachea. The presence of these cells in the upper airway may also allow viral replication upon initial exposure.

Our current understanding about human lung stem/progenitor cells is limited. Recently, a subset of pulmonary $Oct\text{-}4^+$ stem/progenitor cells that could differentiate into pneumocytes has been isolated from neonatal mouse lung (14). Of significance, these mouse stem/progenitor cells express ACE2 and are susceptible to SARS-CoV infection and replication in vitro (14), which at least in part supports our findings. In the adult mouse lung, $CD34^+$ bronchioalveolar stem cells (BASCs) that can differentiate into alveolar epithelia have also been isolated (25). The phenotype of the novel cell subset we identified in the human lung, however, is not entirely compatible to those known mouse lung stem/progenitor cells. For example, the $Oct\text{-}4^+$ stem/progenitor cells isolated from the neonatal mouse lung express cytokeratin and CD15 (i.e., SSEA-1) (14), whereas our cells do not (Fig. 3). The BASCs identified in the adult mouse lung express surfactant (25), which is undetectable in our cells. In addition, instead of being at the bronchioalveolar duct junction where the BASCs are located (25), our cells are scattered in the lung stroma (Fig. 3 A) and in the bronchiolar lining layer (Fig. S6). Nevertheless, we notice that some $CD34^+Oct4^+$ cells in the non-SARS lung are actually juxtaposed to the $cytokeratin^+$ or $surfactant^+$ cells (Fig. 3 A). Therefore, the possibility that these putative stem/progenitor cells in the human lung may differentiate into mature respiratory epithelia or pneumocytes, as in the case in mice, cannot be excluded.

The origin of this novel putative human lung stem/progenitor cell is yet to be determined. In our study, some uninfected $CD34^+Oct4^+$ cells were identified in the alveoli and bronchiolar lining layer of the SARS lung (Fig. 2 and Fig. S6). Furthermore, not all the enrolled non-SARS individuals had these cells in the lung. It is thus likely that these $CD34^+Oct\text{-}4^+$ cells might be blood-borne and recruited into the lung under regulation. This postulation can be supported at least in part by reports that circulation- or bone marrow–derived cells may differentiate into mature respiratory epithelia in animals (26–28), and that preexisting injury may increase recruitment of adult bone marrow–derived cells to the lung, which subsequently give rise to differentiated cells (29). Because $CD34^+Oct4^+$ cells can be found in the non-SARS lung (Fig. 3 A) and can be infected by SARS-CoV ex vivo (Fig. 3 B and Figs. S8 and S9), we regard it unlikely that the presence of these cells in the lung is merely a response to SARS infection. For the same reason, it is also unlikely that these cells are recruited into the lung only as part of an attempt for viral clearance or are the only remaining cells bearing viral antigen by the time of death.

Whether or not these $CD34^+$ cells are also the major target for SARS-CoV in the early phase of infection remains to be investigated. Our ex vivo infection model in part can be a complement to actual early infection. However, in vivo confirmation of the identity of virus-targeted cells in the early phase is difficult because of unavailability of samples from patients who died within 3 d after illness onset or even before the onset. Extrapolation of animal studies to humans for early infection also requires much caution because iatrogenic inoculation with large-volume viral droplets into animals is different from infection in a more natural aerosol form in human settings (30). Moreover, the value and reproducibility of the nonhuman primate model for SARS infection are also highly disputable (31, 32).

Admittedly, the pathogenesis of SARS is still unclear and no satisfactory explanation for a complete picture has been provided by reports in the literature or by this study. Nevertheless, we present clear evidence that putative stem/progenitor $CD34^+Oct4^+$ cells are the major target for SARS-CoV infection in the human lung. With our findings, we postulate that although L-SIGN–mediated viral entry into $cytokeratin^+$ respiratory epithelia leads to viral degradation (13), infection of $CD34^+Oct4^+$ cells may result in cell death (cytopathy) and the production of proinflammatory cytokines or other soluble mediators. The death of the stem/progenitor cells and the resulting local immuno-dysregulation (e.g., cytokine storm from infiltrating immune cells [Fig. S5], including macrophages, and/or from the infected $CD34^+Oct4^+$ cells) may together contribute to alveolar cell damage, loss of repair capacity, and respiratory insufficiency as clinically observed. Isolation and purification of these $CD34^+Oct4^+$ cells are underway to further examine their role in the pathogenesis.

MATERIALS AND METHODS

Lung samples, antibodies, and cRNA probes. Lung autopsy from nine patients fatally infected with SARS were retrieved for the study. Non-SARS lung samples were obtained from 14 adults having lobectomy for lung cancers with approval by the Institutional Review Board of the University of Hong Kong. Mouse anti-SARS CoV nucleocapsid antibody was produced as described previously (13). Other primary antibodies used were listed in Table S1 (available at http://www.jem.org/cgi/content/full/jem.20070462/DC1). Antisense and sense of cRNA probes for FISH and ISH were generated as described previously (13). CD34 cRNA probe corresponding to nucleotides 590–1034 (GenBank accession no. S53910) and Oct-4 cRNA probe corresponding to nucleotides 454–1046 (GenBank accession no. NM002701) were used. ACE2 and L-SIGN (CD209L) probes were described previously (13).

Sequential triple immunostaining on paraffin sections. Sequential immunostaining was performed on 5-μm paraffin sections of formalin-fixed lung samples. Samples were de-paraffinized and rehydrated. After blocking endogenous peroxidase with 0.3% H_2O_2, 0.03% NaN_3 for 30 min at room temperature, mouse anti–surfactant A antibody was added at 4°C overnight. Sections were then incubated with peroxidase-conjugated EnVision plus reagent (anti–mouse, ready to use; DakoCytomation) for 1 h at room temperature and developed with diaminobenzidine chromogen substrate (DakoCytomation). Sections were subjected to microwave heating to block endogenous alkaline phosphatase as well as to inactivate the antibody from the first staining. Mouse anti-SARS CoV nucleocapsid antibody was applied at 4°C overnight, followed by anti–mouse universal immuno-alkaline-phosphatase polymer (ready to use; Nichirei Corporation) for 2 h at room temperature. The color was subsequently developed with a fast red substrate system (Sigma-Aldrich). After immunohistochemical staining, sections were again microwaved to inactivate the antibody from the second staining, followed by incubation with mouse anti-cytokeratin AE1/AE3 at 4°C overnight. Sections were incubated with FITC-conjugated goat anti–mouse IgG (1:400; Sigma-Aldrich) at room temperature for 2 h. Sections were mounted with medium for fluorescence with DAPI (Vector Laboratories). Electronic images of the immunohistochemical and immunofluorescence staining, visualized under a fluorescence microscope (eclipse E600; Nikon), were captured and saved to a computer using the software ACT-1 (Nikon).

IHC, FISH, and ISH on paraffin sections. Sequential IHC was performed similarly as described above. After immunostaining, sections were treated with 0.2 N HCl for 30 min at room temperature to block alkaline phosphatase activity from the previous staining. Sections were then digested with 10 μg/ml proteinase K at 37°C for 15 min. Subsequent FISH and ISH were performed on the same section as described previously (13). The same field as in the IHC, FISH, and ISH images were selected and visualized under the same microscope and saved as electronic images for comparison and analysis of colocalization.

SARS-CoV infection of fresh human lung tissues. Lung tissues were excised from lung cancer patients for ex vivo infection with the approval by the Institutional Review Board of the University of Hong Kong. Fresh lung tissues were cut into small tissue blocks (2–3 mm^3), followed by SARS-CoV (strain GZ50) (33) infection at 5×10^6 $TCID_{50}$ in 1 ml of serum-free RPMI medium at 37°C for 1 h. The culture was then supplemented with 10% fetal bovine serum and further incubated at 37°C for 16 h. Tissue blocks were fixed and processed for subsequent IHC, FISH, and ISH analysis as described above.

Online supplemental material. Fig. S1 shows that L-SIGN is expressed in cytokeratin$^+$ cells. Fig. S2 shows that SARS$^+$ cells do not express surfactant C or T1α. Fig. S3 shows that SARS$^+$ cells do not express cytokeratin or surfactant A. Fig. S4 shows that IHC using an avidin–biotin complex method can result in a false-positive reading for cytokeratin expression in the alveoli. Fig. S5 shows that SARS$^+$ cells do not express most of the common leukocyte markers. Fig. S6 shows that SARS$^+$ cells in bronchioles express both ACE2 and CD34. Fig. S7 shows that SARS-CoV antigen can be found in CD68$^+$ cells. Fig. S8 shows that CD34$^+$Oct-4$^+$ cells in non-SARS lung tissues can be infected by SARS-CoV ex vivo. Fig. S9 shows that SARS-CoV does not infect cytokeratin$^+$ or surfactant A$^+$ cells in fresh lung tissue blocks. Table S1 shows the list of antibodies used. The online supplemental material is available at http://www.jem.org/cgi/content/full/jem.20070462/DC1.

We thank Gordon Stamp for his critical review; J.M. Peiris for discussion; K.F. To, P. Beh, and C.Y. Leung for autopsy materials; E. Yeung for fresh lung samples; K.H. Chan for the anti-SARS antibody; and C. Chan for technical support.

This project was funded by Hong Kong RGC-CERG 7550/05M, Canadian Genetic Diseases Network, and HKU Grant Council Matching Grant 20600436.

The authors have no conflicting financial interests.

Submitted: 5 March 2007
Accepted: 7 September 2007

REFERENCES

1. Peiris, J.S., S.T. Lai, L.L. Poon, Y. Guan, L.Y. Yam, W. Lim, J. Nicholls, W.K. Yee, W.W. Yan, M.T. Cheung, et al. 2003. Coronavirus as a possible cause of severe acute respiratory syndrome. *Lancet*. 361:1319–1325.
2. Ksiazek, T.G., D. Erdman, C.S. Goldsmith, S.R. Zaki, T. Peret, S. Emery, S. Tong, C. Urbani, J.A. Comer, W. Lim, et al. 2003. A novel coronavirus associated with severe acute respiratory syndrome. *N. Engl. J. Med*. 348:1953–1966.
3. Drosten, C., S. Gunther, W. Preiser, S. van der Werf, H.R. Brodt, S. Becker, H. Rabenau, M. Panning, L. Kolesnikova, R.A. Fouchier, et al. 2003. Identification of a novel coronavirus in patients with severe acute respiratory syndrome. *N. Engl. J. Med*. 348:1967–1976.
4. Li, W., M.J. Moore, N. Vasilieva, J. Sui, S.K. Wong, M.A. Berne, M. Somasundaran, J.L. Sullivan, K. Luzuriaga, T.C. Greenough, et al. 2003. Angiotensin-converting enzyme 2 is a functional receptor for the SARS coronavirus. *Nature*. 426:450–454.
5. Peiris, J.S., C.M. Chu, V.C. Cheng, K.S. Chan, I.F. Hung, L.L. Poon, K.I. Law, B.S. Tang, T.Y. Hon, C.S. Chan, et al. 2003. Clinical progression and viral load in a community outbreak of coronavirus-associated SARS pneumonia: a prospective study. *Lancet*. 361:1767–1772.
6. Kuiken, T., R.A. Fouchier, M. Schutten, G.F. Rimmelzwaan, G. van Amerongen, D. van Riel, J.D. Laman, T. de Jong, G. van Doornum, W. Lim, et al. 2003. Newly discovered coronavirus as the primary cause of severe acute respiratory syndrome. *Lancet*. 362:263–270.
7. Haagmans, B.L., T. Kuiken, B.E. Martina, R.A. Fouchier, G.F. Rimmelzwaan, G. van Amerongen, D. van Riel, T. de Jong, S. Itamura, K.H. Chan, et al. 2004. Pegylated interferon-alpha protects type 1 pneumocytes against SARS coronavirus infection in macaques. *Nat. Med*. 10:290–293.
8. Gu, J., E. Gong, B. Zhang, J. Zheng, Z. Gao, Y. Zhong, W. Zou, J. Zhan, S. Wang, Z. Xie, et al. 2005. Multiple organ infection and the pathogenesis of SARS. *J. Exp. Med*. 202:415–424.
9. Shieh, W.J., C.H. Hsiao, C.D. Paddock, J. Guarner, C.S. Goldsmith, K. Tatti, M. Packard, L. Mueller, M.Z. Wu, P. Rollin, et al. 2005. Immunohistochemical, in situ hybridization, and ultrastructural localization of SARS-associated coronavirus in lung of a fatal case of severe acute respiratory syndrome in Taiwan. *Hum. Pathol*. 36:303–309.
10. Li, B.J., Q. Tang, D. Cheng, C. Qin, F.Y. Xie, Q. Wei, J. Xu, Y. Liu, B.J. Zheng, M.C. Woodle, et al. 2005. Using siRNA in prophylactic and therapeutic regimens against SARS coronavirus in Rhesus macaque. *Nat. Med*. 11:944–951.
11. Nicholls, J.M., J. Butany, L.L. Poon, K.H. Chan, S.L. Beh, S. Poutanen, J.S. Peiris, and M. Wong. 2006. Time course and cellular localization of SARS-CoV nucleoprotein and RNA in lungs from fatal cases of SARS. *PLoS Med*. 3:222–239.
12. To, K.F., J.H. Tong, P.K. Chan, F.W. Au, S.S. Chim, K.C. Chan, J.L. Cheung, E.Y. Liu, G.M. Tse, A.W. Lo, et al. 2004. Tissue and cellular tropism of the coronavirus associated with severe acute respiratory syndrome: an in-situ hybridization study of fatal cases. *J. Pathol*. 202:157–163.
13. Chan, V.S., K.Y. Chan, Y. Chen, L.L. Poon, A.N. Cheung, B. Zheng, K.H. Chan, W. Mak, H.Y. Ngan, X. Xu, et al. 2006. Homozygous L-SIGN

(CLEC4M) plays a protective role in SARS coronavirus infection. *Nat. Genet.* 38:38–46.
14. Ling, T.Y., M.D. Kuo, C.L. Li, A.L. Yu, Y.H. Huang, T.J. Wu, Y.C. Lin, S.H. Chen, and J. Yu. 2006. Identification of pulmonary Oct-4+ stem/progenitor cells and demonstration of their susceptibility to SARS coronavirus (SARS-CoV) infection in vitro. *Proc. Natl. Acad. Sci. USA.* 103:9530–9535.
15. Bonnard, C., D.S. Papermaster, and J.-P. Kraehenbuhl. 1984. The streptavidin-biotin bridge technique: application in light and electron microscope immunohistochemistry. *In* Immunolabelling Electron Microscopy. J.M. Polak and I.M. Varndell, editors. Elsevier Scientific Publishers, Amersterdam. 95–111.
16. Bussolati, G., P. Gugliotta, M. Volante, M. Pace, and M. Papotti. 1997. Retrieved endogenous biotin: a novel marker and a potential pitfall in diagnostic immunohistochemistry. *Histopathology.* 31:400–407.
17. Yagi, T., N. Terada, T. Baba, and S. Ohno. 2002. Localization of endogenous biotin-containing proteins in mouse Bergmann glial cells. *Histochem. J.* 34:567–572.
18. Mount, S.L., and K. Cooper. 2001. Beware of biotin: a source of false-positive immunohistochemistry. *Curr. Diagn. Pathol.* 7:161–167.
19. Andrews, R.G., J.W. Singer, and I.D. Bernstein. 1986. Monoclonal antibody 12-8 recognizes a 115-kd molecule present on both unipotent and multipotent hematopoietic colony-forming cells and their precursors. *Blood.* 67:842–845.
20. Simmons, P.J., and B. Torok-Storb. 1991. CD34 expression by stromal precursors in normal human adult bone marrow. *Blood.* 78:2848–2853.
21. Nichols, J., B. Zevnik, K. Anastassiadis, H. Niwa, D. Klewe-Nebenius, I. Chambers, H. Scholer, and A. Smith. 1998. Formation of pluripotent stem cells in the mammalian embryo depends on the POU transcription factor Oct4. *Cell.* 95:379–391.
22. Scholer, H.R., G.R. Dressler, R. Balling, H. Rohdewohld, and P. Gruss. 1990. Oct-4: a germline-specific transcription factor mapping to the mouse t-complex. *EMBO J.* 9:2185–2195.
23. Shinya, K., M. Ebina, S. Yamada, M. Ono, N. Kasai, and Y. Kawaoka. 2006. Avian flu: influenza virus receptors in the human airway. *Nature.* 440:435–436.
24. Tsui, P.T., M.L. Kwok, H. Yuen, and S.T. Lai. 2003. Severe acute respiratory syndrome: clinical outcome and prognostic correlates. *Emerg. Infect. Dis.* 9:1064–1069.
25. Kim, C.F., E.L. Jackson, A.E. Woolfenden, S. Lawrence, I. Babar, S. Vogel, D. Crowley, R.T. Bronson, and T. Jacks. 2005. Identification of bronchioalveolar stem cells in normal lung and lung cancer. *Cell.* 121:823–835.
26. Kotton, D.N., B.Y. Ma, W.V. Cardoso, E.A. Sanderson, R.S. Summer, M.C. Williams, and A. Fine. 2001. Bone marrow-derived cells as progenitors of lung alveolar epithelium. *Development.* 128:5181–5188.
27. Abe, S., C. Boyer, X. Liu, F.Q. Wen, T. Kobayashi, Q. Fang, X. Wang, M. Hashimoto, J.G. Sharp, and S.I. Rennard. 2004. Cells derived from the circulation contribute to the repair of lung injury. *Am. J. Respir. Crit. Care Med.* 170:1158–1163.
28. Krause, D.S., N.D. Theise, M.I. Collector, O. Henegariu, S. Hwang, R. Gardner, S. Neutzel, and S.J. Sharkis. 2001. Multi-organ, multi-lineage engraftment by a single bone marrow-derived stem cell. *Cell.* 105: 369–377.
29. Weiss, D.J., M.A. Berberich, Z. Borok, D.B. Gail, J.K. Kolls, C. Penland, and D.J. Prockop. 2006. Adult stem cells, lung biology, and lung disease. NHLBI/Cystic Fibrosis Foundation Workshop. *Proc. Am. Thorac. Soc.* 3: 193–207.
30. Wang, B., A. Zhang, J.L. Sun, H. Liu, J. Hu, and L.X. Xu. 2005. Study of SARS transmission via liquid droplet in air. *J. Biomech. Eng.* 127:32–38.
31. McAuliffe, J., L. Vogel, A. Roberts, G. Fahle, S. Fischer, W.J. Shieh, E. Butler, S. Zaki, M. St Claire, B. Murphy, and K. Subbarao. 2004. Replication of SARS coronavirus administered into the respiratory tract of African Green, rhesus and cynomolgus monkeys. *Virology.* 330: 8–15.
32. Hogan, R.J. 2006. Are nonhuman primates good models for SARS? *PLoS Med.* 3:e411; author reply, e415.
33. Zhong, N.S., B.J. Zheng, Y.M. Li, Poon, Z.H. Xie, K.H. Chan, P.H. Li, S.Y. Tan, Q. Chang, J.P. Xie, et al. 2003. Epidemiology and cause of severe acute respiratory syndrome (SARS) in Guangdong, People's Republic of China, in February, 2003. *Lancet.* 362:1353–1358.